

## **Porous Biodegradable Polyurethane Scaffolds Prepared by Thermally Induced Phase Separation**

C.A. Martínez-Pérez, P.E. Garcua-Casillas, A. Martínez-Villafaña, A. Duarte Moller, J. Romero-García.

### **Abstract**

Guide regeneration techniques have been recently used to heal soft and hard tissue defects. In this approach, scaffolding plays an important role. Hydroxyapatite (HA) resembles the natural bone mineral and has shown good bone bonding properties. In this work, porous polyurethanes have been prepared by a thermally induced phase separation technique. Freeze drying of the separated polymer/solvent phase produced foams with co-continuous structure of interconnected pores. The microstructure can be controlled by varying polymer concentration, quenching temperature, and co-solvent utilized. This homogenizing technique can lead to the preparation of porous materials with controllable and reproducible morphology. SEM analysis showed that the pore size range varied from a few microns to a few hundred microns. Due to the interconnected pores, and their biocompatibility and bioactivity; they are promising scaffolds for bone – tissue engineering.

### **Introduction**

Recently, biodegradable materials have been proposed in temporary orthopaedic implants<sup>1-5</sup>. A considerable amount of work has been focused in the elaboration of porous materials for guide bone regeneration (GBR), like polyglycolic acid<sup>6</sup>, polylactic acid<sup>7</sup> and polyurethane<sup>8</sup>. These materials should be porous enough to induce and guide cell attachment growth, and tissue regeneration in three dimensions<sup>9, 10</sup>.

For implantation, the porous materials should fulfill a number of requirements among others, high porosity, a large surface area, a large pore size (between 100 $\mu$ m-300 $\mu$ m), and a uniformly distributed and highly interconnected pore structure throughout the matrix<sup>11, 12</sup>. Several methods have been reported to fabricate porous scaffold polymers. Porogen leaching<sup>13, 14</sup>, emulsion freeze drying<sup>15</sup>, expansion in high-pressure gas<sup>16, 17</sup>, and phase separation technique<sup>18, 19</sup> have been reported. The porogen leaching method has been the best known method, and involves the casting of a polymer/porogen composite membrane followed by aqueous washing out of the incorporated porogen. Various porogens such as salts, carbohydrates, and polymers can be used to produce porous materials. The salt-leaching technique was suitable for controlling pore sizes by changing the size of particulates, but residual salts remaining in the scaffolds caused an irregularity problem for cell seeding and culture. Although the freeze drying/salt-leaching techniques have been used to prepare low-density polyurethane materials with a macroporous structure (100-300 $\mu$ m), the large pores were due to the removal of the salt crystals, the pores resulted in an irregular shape, residual salts could remain in the scaffolds, and the use of TIPS was not discussed<sup>5</sup>. The emulsion freeze-drying method often results in a closed cellular structure in the matrix. The expansion technique using a high-pressured CO<sub>2</sub> gas also resulted in a closed pore structure inadequate for cell seeding. The phase separation technique is based on thermodynamic demixing of a homogeneous polymer solvent solution into a polymer rich phase and polymer poor phase, usually by either exposure of the solution to another immiscible solvent or cooling the solution below a binodal solubility curve. In the

<https://cimav.repositorioinstitucional.mx/jspui/>

thermally induced phase separation (TIPS), thermal energy is used as a latent solvent to induce phase separation<sup>19, 20</sup>.

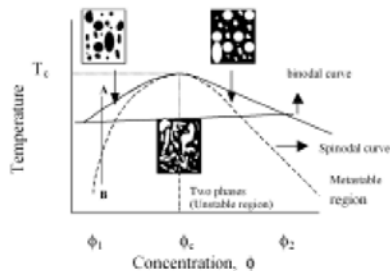


**Figure 1.** A schematic representation of a binary phase diagram of a polymer solution showing the expected morphological variations from liquid – liquid phase separation.

The quenched polymer solution below the freezing point of solvent is subsequently freeze-dried to produce a porous structure. Figure 1 shows a schematic temperature composition phase diagram for a binary polymer/solvent system. Above the binodal curve, a single polymer solution phase is formed. Cooling below the curve, polymer-rich and polymer-poor phases are separated in a thermodynamic equilibrium state to be quenched. For example, when the polymer solution is quenched from point A to point B in Figure 1, the arrested morphology from the position in the metastable zone between the spinodal and binodal curves displays a poor connected stringy or beady structure, which results from a nucleation and growth mechanism.<sup>21</sup> On the other hand, if the system is quenched into the metastable region, the phase separation takes place in a spinodal mechanism, resulting in a microporous interconnected structure.<sup>19-21</sup> The spinodal curve is defined as the line at which the Gibbs free energy of mixing second derivative is equal to zero, and it divides the two-phase region into unstable and metastable regions. Depending upon the location of the quenching end point, two distinctive morphologies can be obtained i.e.; located in the metastable region between binodal and spinodal curves or in the unstable region below the spinodal curve.

<https://cimav.repositorioinstitucional.mx/jspui/>

It is preferable to use the spinodal decomposition for the production of open-pore microcellular foams. Pore size distribution and their interconnectivity are determined by a delicate balance of various parameters such as polymer concentration, quenching route, and solvent/nonsolvent composition<sup>19-21</sup>.

These events occur at the early stage of phase separation, but in the later stage, the coalescence of phase separated droplets continuously proceeds minimizing the interfacial free energy associated with the interfacial area, which is called the coarsening process. This effect is induced by a differential interfacial tension exerted between the two phase separated domains. It was demonstrated that the coarsening process results in pore size enlargement primarily via Ostwald ripening, coalescence, or a hydrodynamic flow mechanism<sup>16, 18</sup>. Thus, the coarsening process should be carefully considered as a kinetic parameter to control the pore morphology of the resulting foams. This effect has been scrutinized in the fabrication of synthetic membranes, because it is of paramount importance in determining the final membrane morphology<sup>22, 23</sup>. To attain macroporous scaffolds, it is desirable to use the coarsening effect, which induces the pore enlargement. The coarsening process, however, concomitantly tends to generate more closed pores; thus, it is important to optimize various TIPS parameters to achieve a macroporous open cellular structure. Large pore size and open cellular structure are critical parameters for cell seeding and neovascularization when implanted in vivo. Polyurethane (PU) has been used in many biomedical applications like vascular prostheses, meniscus reconstruction, and catheters, to mention a few. This versatility is due to high biocompatibility and a wide range of mechanical and physical properties<sup>23-</sup>

<sup>25</sup>.

<https://cimav.repositorioinstitucional.mx/jspui/>

In this study, we investigated the TIPS technique to produce 3D porous biodegradable polyurethane scaffolds by adjusting parameters involved in the TIPS process. 1,4 dioxane was used for solid-liquid phase separation, water was added as a nonsolvent to induce a liquid – liquid phase by lowering the degree of polymer-diluent interaction. Several authors have reported that Ca, P formation on a material's surface in SBF is a indicator of their bioactivity, since bioactive materials bond to bone in vivo through similar surface layer<sup>26,27</sup>. Therefore, in the present study, we also present preliminary results of the calcium phosphate growth on the surface polyurethane previously treated with tetraethoxysilane (TEOS) immersed in 1.5 SBF solution.

## **Experimental Procedures**

### *Porous Polyurethane and Composites Preparation*

Six equivalents of polycaprolactone diol (m.w. 1250) and two equivalents polycaprolactone triol (m.w. 900) were dissolved in 1,4 dioxane and n-hexane as co-solvent followed by the addition of nine equivalents of 1,6 diisocyanatehexane and, as catalyst, 0.5 wt.% of dibutyltin dilaurate was used. Water was added to encourage phase separation. To compare the structures resulting from the variation of solvents, the volume relation of dioxane, nhexane and water were varied as 87:13:0, 93:7:0, 87:0:13, 93:0:7. The homogeneous solutions were quenched under the following conditions: mixture CO<sub>2</sub>/acetone bath (-78°C), and two freezers at -25°C and -15°C, respectively, and then incubated overnight at the quenching temperature. Afterwards, the solutions were placed in a freeze drying apparatus (Labconco Freezone 4.5) connected to a vacuum pressure (0.15 milibar) and the solvent was removed for 48 hours. After freeze-drying, the polymer was cured under reduced atmosphere (26 inHg) at 60°C for 48 h.

<https://cimav.repositorioinstitucional.mx/jspui/>

HA 5% wt. was added to a polymeric solution before freezing to prepare the composites. The mixture was stirred magnetically for 15 min.

#### *Preparation of SBF Solution*

The simulated body fluid (1.5 SBF) which had approximately 1.5 times higher ionic concentrations than human blood plasma and was prepared according to literature<sup>28</sup> by dissolving reagent-grade NaCl, NaHCO<sub>3</sub>, KCl, K<sub>2</sub>HPO<sub>4</sub>·3H<sub>2</sub>O, MgCl<sub>2</sub>·6H<sub>2</sub>O, CaCl<sub>2</sub> and Na<sub>2</sub>SO<sub>4</sub> in ionexchange distilled water. The solution was buffered at pH 7.25 with tris (hydroxymethyl) aminomethane ((CH<sub>2</sub>OH)<sub>3</sub>CNH<sub>2</sub>) and 1 M hydrochloric acid (HCl) at 37°C.

#### *TEOS and SBF Treatment*

Rectangular substrates (2 x 2 x 1 cm<sup>3</sup>) of polyurethane were cut and then soaked in 20 ml of 1M HCl for three min. in order to increase the number of polar groups and increase the affinity of the silicate ions to the substrate<sup>28</sup>. After the HCl treatment, substrates were washed with distilled water and dried at room temperature, each substrate was soaked in 40 ml. of (TEOS, 99%) the flask was kept at 60°C for 2 h. After cooling the flask, substrates were filtered out and washed with ethyl alcohol and then each substrate was soaked in 1.5 SBF at 37°C in the polystyrene bottle for different periods for making the apatite nuclei grow on the surface of the substrate in situ. The 1.5 SBF solution was renewed every day. After that, the substrate was washed moderately with distilled water and dried at room temperature.

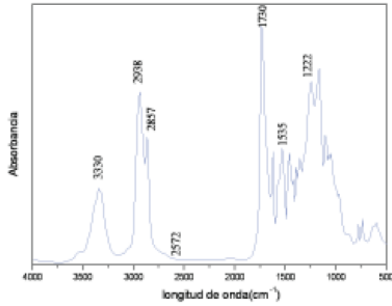


**Figure 2.** FT-IR of a polyurethane sample.

## Results and discussion

A scaffold material for tissue engineering should have a high porosity and an appropriate pore size. In this work, the solid-liquid phase separation of PU/dioxane/nonsolvent and subsequent sublimation of the solvent has been used to obtain highly porous polyurethane. The FT-IR spectra of the PU developed is presented in Figure 2. The spectrum shows the characteristic peaks for polyurethane like  $3330\text{ cm}^{-1}$  which are attributed to the vibration stretching mode of N-H; at  $1730\text{ cm}^{-1}$  non-hydrogen bonded urethane C=O stretch, at  $1535\text{ cm}^{-1}$  corresponding to the stretching mode of urethane N-H bonding + C-N; and at  $1222\text{ cm}^{-1}$  the peak is attributed to C-N stretching.

Freeze-drying of a polymer solution is a process in which the solvent is removed by sublimation from the frozen material so that it leaves a porous structure. The density of the resulting porous polymer was determined by concentration of the polymer in the solution; and the morphology of the foam is determined by phase separation. Phase separation can be divided into liquid-liquid phase separation (which may occur prior to freezing of the solvent) and liquid-solid phase separation (which occurs when the solvent freezes). Adding a co-solvent or non-solvent to the solution may induce liquid-liquid phase separation<sup>19</sup>. Figure 3 shows SEM pictures of different morphologies of a

<https://cimav.repositorioinstitucional.mx/jspui/>

35% (w/v) (polymer/solvent) PU prepared in pure dioxane and quenched at different temperatures. When the polymer solution was quenched at  $-78^{\circ}\text{C}$ , a microcellular pore structure was formed, suggesting that the quenched state of the polymer solution was located within the unstable region, see Figure 1. The cell sizes in the scaffolds increased at  $-25^{\circ}\text{C}$ . The microstructure was bead-like and ladder-like, respectively. The anisotropic morphologies were likely developed by a solid-liquid phase separation, in which preferential crystallization of pure dioxane predominantly occurred in the direction of heat transfer.

The morphology of polyurethane 35% (w/v) prepared in varying solvent volume ratios of dioxane and n-hexane as co-solvent is shown in Figure 4 and 5. We can see that increases in the ratio of n-hexane and the quenching temperature, results in an increase of the spaces,. The nhexane improves a solid –liquid phase separation and the morphologies obtained were a bead-string like structure. The formation of this structure suggests that a nucleation and growth mechanism proceeded at this polymer concentration as a major TIPS pathway.

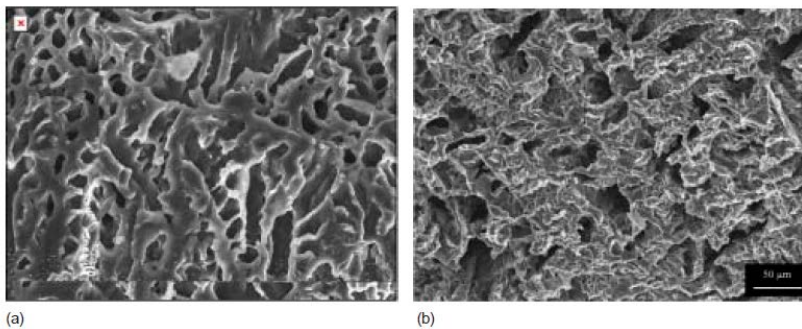


**Figure 3.** SEM images of the cross section of polyurethane produced by quenching 35%(w/v) polymer solution in pure dioxane at  $-78^{\circ}\text{C}$ (a) and  $-25^{\circ}\text{C}$ .

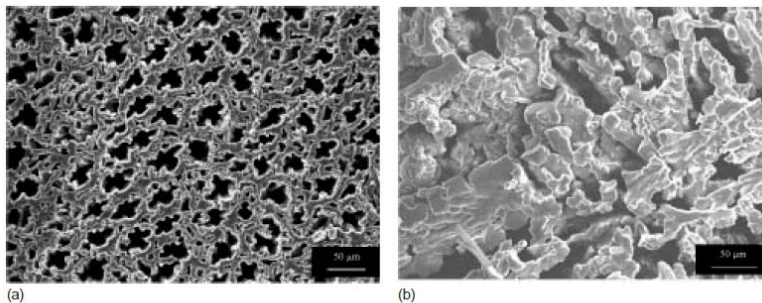


**Figure 4.** SEM images of cross section of polyurethanes as a function of the quenching temperature prepared by 35% (w/v) polymer in dioxane/c-hexane (86:14 v/v) quenched at a)  $-78^{\circ}\text{C}$ ; b)  $-15^{\circ}\text{C}$ .

In order to improve liquid-liquid phase separation, water was added as non-solvent in different ratios. Figure 6 shows SEM pictures of different morphologies of 35% (w/v) PU prepared in varying volume ratios of dioxane and water at different quenched temperatures. In general, the morphologies showed an open cellular microporous structure. The increasing amount of water in the solvent mixture tended to generate large cellular pore sizes. This was probably caused by the fact that as the non-solvent volume fraction increased, a weaker polymer-diluent interaction might induce the formation of polymer poor phase with greater droplet domains.

This can be explained by the above mentioned coarsening effect, in which a phase-separated polymer-poor (solventrich) droplets coalesce to form larger droplet domains at the later stage of phase separation. Since the coarsening effect reflects a kinetic behaviour towards the thermodynamic minimization of interfacial energy, one can manipulate the cellular structure by arresting the phase separation process. In this study, the coarsening effect decreased with the decrease in the quenching temperature.

It is worth to noting that even though the solid  $\text{CO}_2$ / acetone quenched scaffolds exhibited a microcellular morphology, their closed cell structures were somewhat different from the typical bicontinuous morphology produced by a spinodal decomposition mechanism, as shown in Figure 1. As the polymer solution was

<https://cimav.repositorioinstitucional.mx/jspui/>

incorporated into the solid CO<sub>2</sub>/acetone mixture, it is conceivable that an instantaneous heat gradient, although presumably of short duration, developed in the direction from the contacting mold surface to the core region of the quenched polymer sample. This would create different phase-separated morphologies from the centre towards the surface in the resultant scaffolds by exerting locally different phase arresting time scales on the spinodal decomposition. Thus, until the final phase arresting occurred, the coarsening effect was likely to play a critical role in the core region and the surface. This effect was expected to be more pronounced in a large dimensional sample. From this reasoning, the prepared scaffolds developed microporous surface skin structure, whereas in the core region macroporous structure was developed.

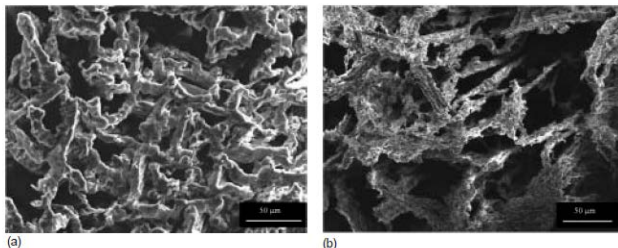


**Figure 5.** SEM images of cross section of polyurethanes as a function of quenched temperature prepared by 35%(w/v) polymer in dioxane-hexane (70:30 v/v), quenched at a) -25°C; b) -15°C.

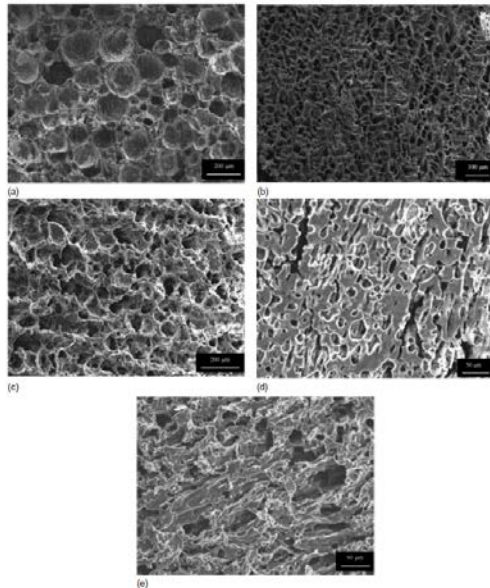


**Figure 6.** SEM images of the cross section of PU scaffolds as a function of quenched temperature and solvent/nonsolvent volume ratio. The scaffolds were prepared by quenching a 35%(w/v) polymer solution under the following conditions: -78°C(a,d); -25°C (b,e); -15°C(c,f). The volume ratios of dioxane and water were 84/16 (a,b,c); 93/07 (d,e,f).

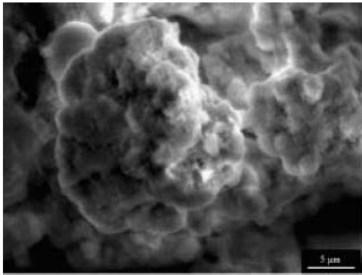


**Figure 7.** (a) SEM picture of TEOS treated polyurethane after immersion in 1.5 SBF solution for 2336 h.

In order to have an indicator of the PU biocompatibility; the samples were treated with tetraethoxysilane and then were immersed in 1.5 SBF. A SEM picture of TEOS treated polyurethane after immersion in SBF during 336 h is shown in Figure 7. It can be form apatite nuclei onto functionalized polyurethane after 24 h. after the nucleation of sufficient number of apatite nuclei the surface is covered by calcium phosphate particles accompanied by a secondary nucleation over the initial layer.

The Ca-P layer formed on a polymer's surface is composed of spherulites with very fine crystallites, suggesting a high Ca,P nucleation rate. Some spherulites were formed directly on the surface of other growing spherulites or their interface. This type of occurrence suggests that the front of a growing layer is also preferential nucleation site for other spherulites. Figure 8 shows the set of EDAX patterns of the SBF-treated samples indicate the presence of some sodium and chlorine, from the SBF solution. Magnesium and potassium were also detected. These elements especially magnesium, could instead, be incorporated in the apatite structure and replace calcium. The silicon peak disappears as the time of immersion increases; it was almost fully dissolved due to mechanism based on the hydration, formation of silanol groups and consequent nucleation of the Ca-P particles. The Ca/P value of the coatings were determined by ICP and EDAX and was closely 1.6 after 336 h, less than 1.67 Ca/P value of pure

<https://cimav.repositorioinstitucional.mx/jspui/>

hydroxyapatite due to the incorporation of other ions. The formation of apatite in the polymer surface is an indicator of its bioactivity.

## Conclusions

Highly porous poly(urethanes) can be fabricated by using a thermally induced phase technique. It is possible to control porosity and the morphology by varying the polymer concentration, quenching temperature and the co-solvent utilized. The better structure according to the mentioned characteristics was obtained using water as a non solvent in the ratio of 86:14 dioxane/water and quenched temperatures of  $-25$  and  $-15^{\circ}\text{C}$ . These biodegradable scaffolds materials coated with bonelike apatite have a great potential as bone – repairing materials, due to high bioactivity favourable to bond to bone chemically and to allow the growth of connective tissue through the porous of the material.

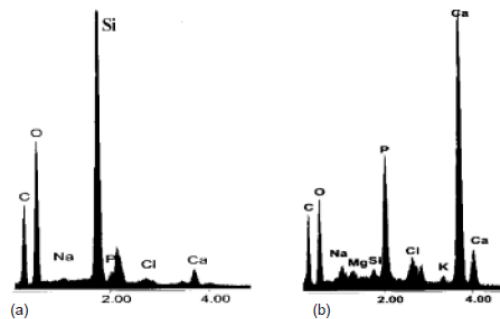


Figure 8. EDAX patterns of TEOS treated samples immersed in 1.5SBF after: (a) 24 h immersion; (b) 336 h. immersion.

## References

1. C. Chaput, E.A. DesRosiers, M. Assad, M. Brochu, L.H. Yahia, A. Selmani, C.-H. Rivard, *Advances in Materials Science and Implant Orthopaedic Surgery*, Luwer Academic Publishers, Dordrecht, The Netherlands, p. 229, 1995.
2. A. G. Mikos, Y. Bao, L.M. Cima, D. Ingber, J.P. Vacanti, R.J. Langer, *J. of Biomed. Mat. Res.*, 27, p. 183, 1993.

<https://cimav.repositorioinstitucional.mx/jspui/>

3. A.G. Mikos, Sarakinos, G.S.M. Leite, J.P. Vacanti, R. Langer, *Biomaterials*, 14, p. 323, 1993.
4. G.J. Beumer, C.A. van Blitterwijk, D. Bakker, M. Ponce, *Biomaterials*, 14, p. 598, 1993.
5. J.H. de Groot, A.J. Nijenhuis, P. Bruin, A.J. Pennings, R.P.H. Veth, J. Klompmaker, and H.W.B. Jansen, *Colloid and Polymer Science*, 268 n. 12, p. 1073, 1990.
6. K.A. Athanasiou, G.G. Nidederauer, C.M. Agrawal, *Biomaterials*, 17, p. 93, 1996
7. B. Immirzi, M. Malinconico, G. Orsello, S. Portofino, M.G. Volpe, *J. Mater. Sc.* 34, p. 1625, 1999.
8. M. Sheth, R.A. Kumar, D. Vipul, R.A. Gross, S.P. Mccarthy, *J. Appl. Polym. Sci.*, 66, p. 1495, 1997.
9. N. Ignjatović, S. Tomic, M. Dakic, M. Miljkovic, M. Plavsic, D. Uskokovic, *Biomaterials*, 20, p. 809, 1999.
10. S. Jin, K.J. Gonsalves, *J. Mater. Sc. Mater. Med.*, 10, p. 363, 1999.
11. T. C. Lindholm, T.J. Gao, T.S. Lindholm, *Int. J. Oral Maxillofac. Surg.*, 23, p. 306, 1994.
12. A.C.A. Wan, E. Khor, G.W.J. Hastings, *J. Biomed. Mater. Res. (Appl. Biomater)*, 38, p. 235, 1997.
13. L. Freed, J.C. Marquis, A. Nohria, J. Emmanue, A.G. Mikos, *J. Biomed. Mater. Res.*, 1993, 27:11-23.
14. A.G. Mikos, G. Sarakinos, S.M. Leite, J.P. Vacante, R. Lauger, *Biomaterials*, 1993; 14: 323-330.
15. K. Whang, C.H. Thomas, K.E. Healy, G. Nuber, *Polymer*, 1995; 36, 837-842.

<https://cimav.repositorioinstitucional.mx/jspui/>

16. D.J. Mooney, D.F. Baldwin, N.P. Such, J.P. Vacanti, R. Langer, *Biomaterials*, 1996;17, 1417-1422.
17. L.D. Harris, B.S. Kim, D.J. Mooney, *J. Biomed. Mater. Res.* 1998; 42, 396-402.
18. H. Lo, S. Kadiyala, E. Guggino, K.W., Leong, *J. Biomed. Mater. Res.*, 1996; 30, 475-484.
19. N. Young Soun, P. Tae Gwan, *J. Biomed. Mater. Res.*, 1999; 47, 8-17.
20. S.W. Song, J.M. Torkelson, *Macromolecules*, 1994; 27:6389-6397.
21. F. Jun Hua, G. Eun Kim, J. Doo Lee, Y. Keun Son, D. Sung Lee, *J. Biomed Mater. Res.*, 2002; 63, 161-167.
22. C. Schugen, V. Maguet, C. Grandfils, R. Jerome, P. Teyssie, *J. Biomed. Mater. Res.* 1996, 30 449-461.
23. M. Szycher, A.A. Siciliano, and A.M. Reed, "Polyurethane Elastomers in Medicine," *Polymeric Biomaterials*, ed. S. Dumitriu, Marcel Decker, Inc., New York, NY., p. 233, 1994.
24. S. Worley, R. Marchand, C. Lavallée, *Biomaterials*, 11, p. 97, 1990.
25. T.V. Chirilia, I.J. Constable, G.J. Crawford, S. Vijayasekaran, D.E. Thompson, Y.C. Chen, W.A. Fletcher, B.J. Griffin, *Biomaterials*, 14, p. 26, 1993.
26. M. Neo, T. Nakamura, T. Yamamuro, C. Ohtsuki, T. Kokubo, and Y. Bando, *J. Biomed. Mater. Res.*, 26, p. 1419, 1992.
27. M. Neo, S. Kotani, Y. Fujita, T. Yamamuro, Y. Bando C. Ohtsuki, and T. Kokubo, "Differences in Ceramic-bone Interface Between Surface-active Ceramics and Resorbable Ceramics: A Study by Scanning and Transmission Electron Microscopy," *J. Biomed. Mater. Res.*, 26, p. 452, 1992.

<https://cimav.repositorioinstitucional.mx/jspui/>

28. M. Tanahashi, T. Yao, T. Kokubo, T. Miyamoto, M. Minnoda, T. Nakamura, T. Yamamuro, J. Mater. Sc. Mater. Med., 6, p. 319, 1995.